β-Phosphatoxyalkyl Radical Reactions: Competing Phosphate Migration and Phosphoric Acid Elimination from a Radical Cation–Phosphate Anion Pair Formed by Heterolytic Fragmentation

ARTICLE *in* JOURNAL OF THE AMERICAN CHEMICAL SOCIETY · NOVEMBER 1999

Impact Factor: 12.11 · DOI: 10.1021/ja991012r

β-Phosphatoxyalkyl Radical Reactions: Competing Phosphate Migration and Phosphoric Acid Elimination from a Radical Cation−Phosphate Anion Pair Formed by Heterolytic Fragmentation

Martin Newcomb,*[,1a] John H. Horner,[1a] Patrick O. Whitted,[1a] David Crich,*[,1b] Xianhai Huang,[1b] Qingwei Yao,[1b] and Hendrik Zipse*[,1c]

Contribution from the Department of Chemistry, Wayne State University, Detroit, Michigan, 48202, Department of Chemistry, University of Illinois at Chicago, 845 West Taylor Street, Chicago, Illinois 60607-7061, and Institute für Organische Chemie, Ludwig-Maximilians-Universität, Butenandtstrasse 5−13, D-81377, München, Germany

Received March 29, 1999. Revised Manuscript Received September 30, 1999

Abstract: β-Phosphatoxyalkyl radical reactions were studied experimentally and computationally. The 1,1-dibenzyl-2-(diphenylphosphatoxy)-2-phenylethyl radical (**1**) reacted to give the migration product 2-benzyl-2-(diphenylphosphatoxy)-1,3-diphenylpropyl radical (**2**) and the elimination product 2-benzyl-1,3-diphenylallyl radical (**3**) in a variety of solvents. A modest kinetic solvent effect for reactions of **1** was found. Variable temperature studies in THF and acetonitrile gave Arrhenius functions with similar log *A* terms; the entropies of activation are ∼−5 eu. A deuterated analogue of radical **1** reacted in THF and acetonitrile with rate constants indistinguishable from those of **1**, but the ratio of products **2**:**3** increased for the deuterated radical requiring kinetic isotope effects (KIEs) in reactions following the rate-limiting step. In aqueous acetonitrile solutions, the β,β-dibenzylstyrene radical cation (**4**) was detected as a short-lived intermediate, and the rate constants for formation of **3** and **4** indicated that both species derived from a common intermediate. The 1,1-dimethyl-2-(dimethylphosphatoxy)ethyl radical (**C1**) was studied computationally. Transition states for concerted phosphate migrations and phosphoric acid elimination were found with energies in the order [1,2]-migration < [1,3]-elimination < [3,2]-migration; each transition state was more polarized than radical **C1**. A transition state for homolytic fragmentation of **C1** to give 2-methylpropene and the dimethylphosphatoxyl radical could not be found, but the reaction from the ensemble of these two entities to give the 2-methylallyl radical and phosphoric acid was followed computationally. KIEs and solvent dielectric effects were computed for each concerted reaction of **C1**. The results indicate that radical **1** reacts in all solvents studied by a common pathway involving initial heterolysis. The first-formed contact pair of radical cation **4** and diphenyl phosphate anion collapses to products **2** and **3** and, as a minor process, evolves to diffusively free radical cation **4** in aqueous acetonitrile solutions. A model for heterolytic fragmentation of β-ester radicals involving contact and solvent-separated ion pairs is presented.

β-Phosphatoxyalkyl radicals have received increased attention in recent years in large part because such species are implicated in DNA degradation by anti-cancer agents such as bleomycin and enediyne antibiotics.[2] Reactions of these radicals are complex.[3] They can react to give elimination products, substitution products, or rearrangement products (Figure 1), and multiple reaction pathways to each product are possible. For example, initial heterolysis of the β-phosphatoxyalkyl radical to a radical cation and phosphate anion followed by proton transfer, nucleophilic capture of the radical cation, or recombination would produce the various products. Alternatively, pathways that do not involve radical cation formation are possible; these include concerted eliminations and migrations and direct nucleophilic addition at the radical center with displacement of the β-phosphate in a reaction that is the open-shell analogue of an S_N2' reaction. In a seeming paradox, the consensus views of the mechanisms of β-phosphatoxyalkyl radical reactions as presented in a recent review[3] have been selected from both types of processes. Some details are presented in the Discussion, but we note here that the general view of phosphate migrations is that they are concerted, whereas elimination and substitution reactions are thought to involve initial heterolysis to a radical cation and phosphate anion.

Our respective groups have addressed the mechanisms of β-phosphatoxyalkyl radical reactions from experimental and computational perspectives. Stereochemical labeling studies implicated concerted migration reactions.[4,5] Laser flash photolysis (LFP) kinetic studies of β-phosphatoxyalkyl radicals coupled with product analyses found that phosphate migrations, an elimination and a nucleophilic substitution reaction proceeded without diffusively free radical cation intermediates, and the kinetic results were considered to be most consistent with concerted processes.[6,7] Low energy pathways for concerted

(1) (a) Wayne State University. (b) University of Illinois at Chicago. (c) Ludwig-Maximilians-Universität.

(2) Pogozelski, W. K.; Tullius, T. D. *Chem. Rev.* **1998**, *98*, 1089−1107.

(3) Beckwith, A. L. J.; Crich, D.; Duggan, P. J.; Yao, Q. W. *Chem. Rev.* **1997**, *97*, 3273−3312.

(4) Crich, D.; Yao, Q. W. *J. Am. Chem. Soc.* **1993**, *115*, 1165−1166.

(5) Crich, D.; Yao, Q. W.; Filzen, G. F. *J. Am. Chem. Soc.* **1995**, *117*, 11455−11470.

(6) Choi, S. Y.; Crich, D.; Horner, J. H.; Huang, X. H.; Martinez, F. N.; Newcomb, M.; Wink, D. J.; Yao, Q. W. *J. Am. Chem. Soc.* **1998**, *120*, 211−212.

10.1021/ja991012r CCC: $18.00
Published on Web 00/00/0000 PAGE EST: 9.2

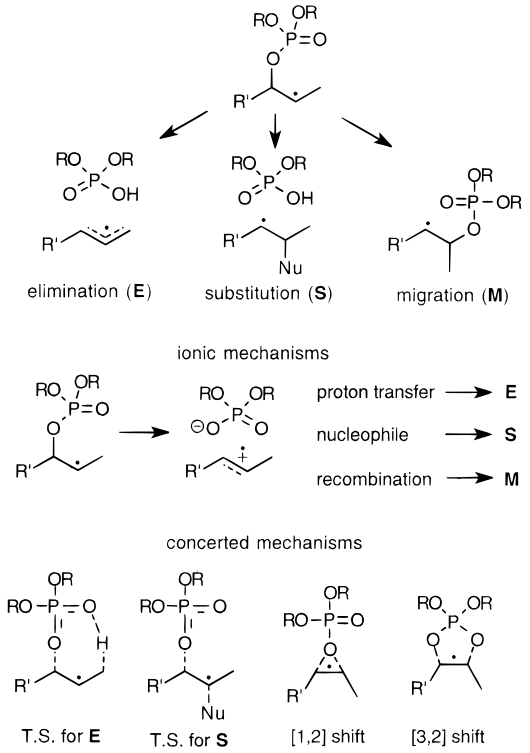

Figure 1. Reactions of β-phosphatoxyalkyl radicals.

[1,2]- and [3,2]-phosphate shifts, for concerted syn-[1,3] eliminations, and for nucleophilic β-displacement of phosphate were found computationally.[8]

In a preliminary publication,[6] we reported that the 1,1-dibenzyl-2-(diphenylphosphatoxy)-2-phenylethyl radical (**1**) reacts by a combination of migration and elimination reactions to give product radicals **2** and **3**, which, according to the consensus views,[3] arise from completely different mechanisms. This system is, thus, well-suited for mechanistic scrutiny. We report here details of LFP studies of reactions of radical **1** and a deuterated analogue (**1**-d_{14} with perdeutero benzyl groups) and computational studies of a model of radical **1** that provide barriers for various concerted processes in a common system. Consistent Arrhenius log *A* parameters for reactions of **1** and smooth increases in rates with solvent polarity increases implicate a common mechanism for migration and elimination reactions in both low and high polarity solvents. The absence of a kinetic isotope effect (KIE) in the overall reactions of **1** and the detection of radical cation **4** in reactions conducted in aqueous solutions indicate that the mechanism involves initial heterolytic fragmentation. We discuss a mechanistic model for β-phosphatoxyalkyl radical reactions involving reactions in ion pairs that appears to be consistent with extant results.

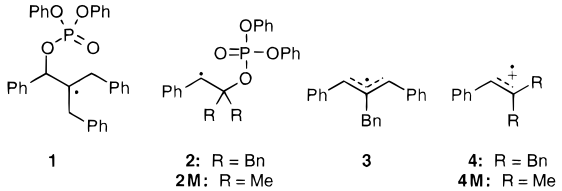

Results

LFP Studies. All radicals studied in this work were produced by 355 nm (third harmonic of a Nd:YAG laser) photolysis of

Scheme 1

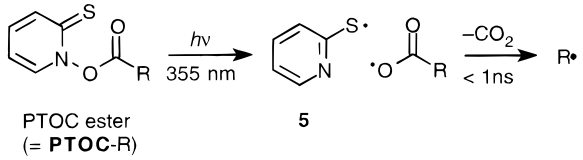

Scheme 2[a]

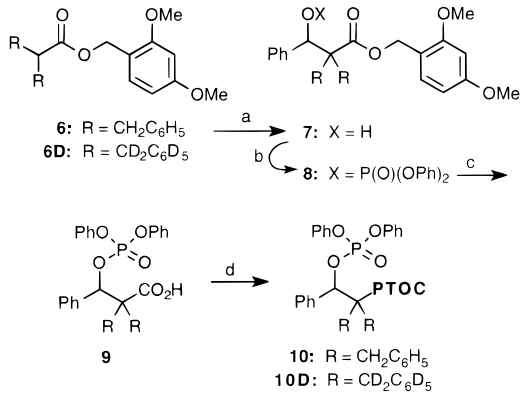

[a] (a) (1) LDA, (2) benzaldehyde; (b) $ClP(O)(OPh)_2$; (c) CAN; (d) 2,2′-dipyridyl disulfide bis-*N*,*N*′-oxide, Bu_3P.

PTOC ester precursors. These precursors, which are isoelectronic with diacyl peroxides, have long wavelength absorbances with λ_{max} at about 360 nm and are cleaved with high efficiency. The photolysis initially gives the pyridine-2-thiyl radical (**5**), which has a broad long wavelength absorbance with λ_{max} at 490 nm,[9] and an acyloxyl radical, but acyloxyl radicals decarboxylate with subnanosecond lifetimes to give the desired alkyl radicals (Scheme 1). In subsequent schemes, the pyridine-2-thioneoxycarbonyl moiety is represented as **PTOC**, and the short-lived intermediate acyloxyl radicals are not shown.

The LFP work was made possible by synthetic advances that permitted the preparation of β-phosphatoxycarboxylic acids, the requisite precursors to the PTOC esters. Such compounds provide a synthetic challenge because phosphoric acid elimination to give acrylate products is facile, and, in fact, β-phenyl-β-phosphatoxycarboxylic acids could only be prepared when the α-carbon was quaternary. The synthetic sequence for the precursor to radical **1**, PTOC ester **10**, is shown in Scheme 2. The key feature is acid protection with 2,4-dimethoxybenzyl alcohol which was removed oxidatively with reasonable efficiency.

Low-temperature condensation of the lithium enolate of the 2,4-dimethoxybenzyl ester of 2-benzyldihydrocinnamic acid (**6**) with benzaldehyde gave the aldol product **7** in good yield. This was then treated with diphenylphosphoryl chloride to give the stable phosphate ester **8**, which could be purified by silica gel chromatography. The 2,4-dimethoxybenzyl ester was removed by treatment with ceric ammonium nitrate. The β-(phosphatoxy-)alkanoic acid **9** so-obtained was relatively unstable, and attempted passage over silica gel resulted in the formation of a β-lactone. Thus, after removal of the 2,4-dimethoxybenzaldehyde byproduct, by extensive washing with sodium bisulfite, the crude acid **9** was immediately converted to the PTOC ester **10** by treatment with 2,2′-dipyridyl disulfide *N*,*N*′-dioxide. This method of PTOC formation[10] was selected from the many available[11] as it enabled their rapid elution from silica gel ahead

(7) Choi, S.-Y.; Crich, D.; Horner, J. H.; Huang, X.; Newcomb, M.; Whitted, P. O. *Tetrahedron* **1999**, *55*, 3317−3326.
(8) Zipse, H. *J. Am. Chem. Soc.* **1997**, *119*, 2889−2893.
(9) Alam, M. M.; Watanabe, A.; Ito, O. *J. Org. Chem.* **1995**, *60*, 3440−3444.
(10) Barton, D. H. R.; Samadi, M. *Tetrahedron* **1992**, *48*, 7083−7090.
(11) Crich, D.; Quintero, L. *Chem. Rev.* **1989**, *89*, 1413−1432.

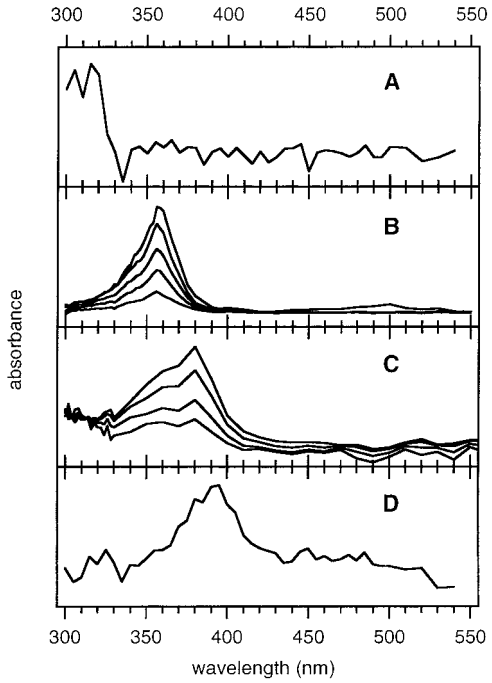

Figure 2. (A) Spectrum of radical **2M** in acetonitrile; see text for an explanation of the method. (B) Time-resolved decay spectrum of radical **3** in acetonitrile. (C) Time-resolved decay spectrum of radical cation **4M** produced by photoejection from the corresponding styrene in acetonitrile. (D) Spectrum of radical cation **4** produced by triplet chloranil oxidation of the corresponding styrene; see text for an explanation of the method.

of any more polar reagents and byproducts. The procedure was repeated with acid **6D** containing perdeuterated benzyl groups to give **10D**. PTOC ester **11**, the precursor to benzylic radical **2M**, was prepared by an analogous route involving aldol condensation of 2,4-dimethoxybenzyl phenylacetate with acetone, followed by phosphorylation and deprotection. PTOC ester **12**, the precursor to radical **3**, was prepared as a mixture of diastereomers from a mixture of (*E*)- and (*Z*)-3-benzyl-2,4-diphenyl-3-butenoic acids resulting from carboxylation of the corresponding allyllithium reagent.

The putative products from reactions of radical **1** are the benzylic radical **2**, the diphenylallylic radical **3**, and the styrene radical cation **4**. One could anticipate from literature reports that the UV spectra of **2**−**4** would be distinct, but authentic spectra were desired for unambiguous identifications of the products. We obtained spectra of radicals **2M** (a model for **2**) and **3** and radical cation **4**.

Figure 2A shows the spectrum of benzylic radical **2M** in acetonitrile obtained in the following manner. Photolysis of PTOC precursor **11** gave **2M** and byproduct radical **5**, but because the extinction coefficient for the benzylic radical is relatively small, the prominent signals were from formation of **5** and bleaching of the precursor. We have observed that the rate of decay of radical **5** is not affected by the presence of oxygen; apparently this radical decays mainly by recombination reactions. The benzylic radical **2M** will react rapidly with oxygen, but it is relatively persistent in the absence of oxygen. Therefore, decay spectra from He-sparged and nonsparged solutions of precursor **11** were obtained over the period 0.2−4.5 μs, and the decay spectrum for the nonsparged solution was subtracted from that of the sparged solution. This subtraction procedure removed the absorbance signals from **5** and the bleaching signals from the precursor to leave the residual spectrum of **2M** that is shown in Figure 2A. The absorbance for **2M** with a λ_{max} at 320 nm is typical for benzylic radicals,[12] and the β-phosphate group obviously has little effect on the position of the absorbance.

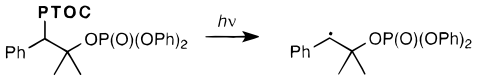

11 **2M**

Allylic radical **3** was produced from the PTOC ester precursor **12**. Figure 2B shows a time-resolved decay spectrum of this radical as it reacts relatively slowly. The spectra were obtained by subtracting the spectrum at 250 μs from those at earlier (3−100 μs) times.[13] The extinction coefficient for radical **3** is so large that signals from radical **5** do not obscure the spectrum, although a small amount of decay at 490 nm from radical **5** can be seen in the figure. The spectrum for allylic radical **3** with λ_{max} at 354 nm is similar to that previously reported for the 1,3-diphenylallyl radical.[14]

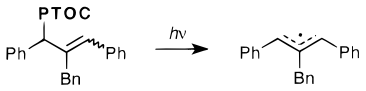

12 **3**

Styrene radical cations can be obtained by LFP methods by direct photoejection from the styrene or by chemical oxidation by a triplet state oxidant produced by photolysis. They have strong absorbances in the 350−390 nm region and weaker absorbances at longer wavelengths (>580 nm).[15] Direct photoejection from 2-methyl-1-phenylpropene in CH_3CN by 266 nm irradiation gave the time-resolved spectrum of radical cation **4M** shown in Figure 2C; radical cation **4M** produced in trifluoroethanol also has an absorbance centered at 380 nm.[15] When the same conditions were used with 2-benzyl-1,3-diphenylpropene, however, the observed spectrum was due to multiple species. The spectrum had λ_{max} at ∼355 nm with a shoulder at 380−390 nm that decayed rapidly relative to the absorbance at 355 nm, and after several μs, the observed spectrum was similar to that from allylic radical **3**. Apparently, the predominant absorbance was due to **3** formed instantly on the nanosecond time scale by a deprotonation reaction occurring in the contact ion pair of radical cation **4** and the acetonitrile radical anion.

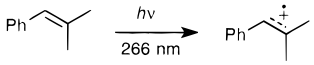

4M

Production of radical cation **4** by oxidation of the corresponding styrene with triplet excited chloranil (formed by 355 nm excitation) in CH_3CN solution was possible, but the spectra were complex. The relatively long-lived chloranil triplet has

(12) Chatgilialoglu, C. In *Handbook of Organic Photochemistry*; Scaiano, J. C., Ed.; CRC Press: Boca Raton, FL, 1989; Vol. 2, pp 3−11.

(13) At short reaction times (<1 μs), a fast dynamic process was observed for radical **3**. The first-observed spectrum had λ_{max} at 360 nm, but a rapid 6 nm hypsochromic shift of λ_{max} and a slight (∼10%) increase in absorbance occurred with a rate constant of 2×10^6 s^{-1} at 20 °C. Given the low concentrations of precursor and radicals in the LFP experiments, this dynamic process cannot be due to radical−radical or radical−precursor reactions, and we ascribe it to a unimolecular process. Apparently, radical **3** was initially produced in a nonequilibrium distribution of conformations and relaxed rapidly by bond rotation.

(14) Miranda, M. A.; Perez-Prieto, J.; Font-Sanchis, E.; Kónya, K.; Scaiano, J. C. *J. Org. Chem.* **1997**, *62*, 5713−5719.

(15) Johnston, L. J.; Schepp, N. P. *J. Am. Chem. Soc.* **1993**, *115*, 6564−6571.

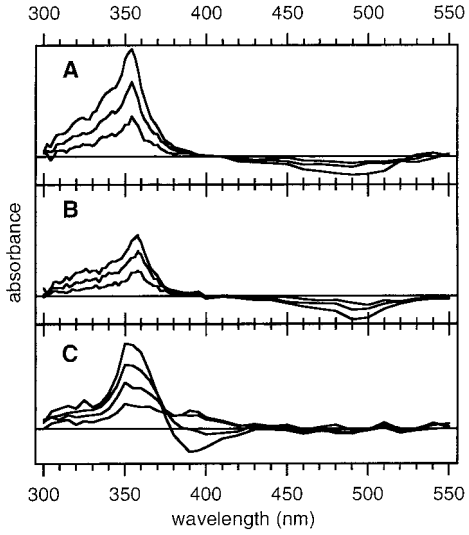

Figure 3. Time-resolved spectra from reaction of radical **1**-d_0 (A) and radical **1**-d_{14} (B) in acetonitrile at 19.8 °C; the spectra show signal evolution over 7.6 μs with the signals at 0.8 μs subtracted to give a baseline. (C) Time-resolved spectrum from reaction of radical **1** in water/acetonitrile (1:1, v:v) at 22 °C; signal evolution is over 1.0 μs with the spectrum at 100 ns subtracted to give a baseline; signals from 300 to 370 nm are growing, and the signal centered at 390 nm is decaying after rapid growth.

broad absorbances centered at 370 and 510 nm,[16] and the chloranil radical anion, formed upon oxidation of the styrene, absorbs at 320 and 440 nm.[17] In addition, a persistent signal with λ_{max} at ~355 nm, apparently due to allylic radical **3**, was present in the spectra. The spectrum of radical cation **4** shown in Figure 2D was obtained by subtracting the spectrum at 45 μs from that at 5 μs. Under the conditions employed, the chloranil triplet signals had decayed completely by 5 μs, leaving signals from the chloranil radical anion, allylic radical **3,** and radical cation **4**. In the period 5−45 μs, signals from radical cation **4** decayed more rapidly than those from other species. Because the residual spectrum at 45 μs still contained the signal from **3**, the difference spectrum in Figure 2D is due mainly to **4** (λ_{max} at 390 nm) and the chloranil radical anion (small absorbances at 320 and 440 nm).

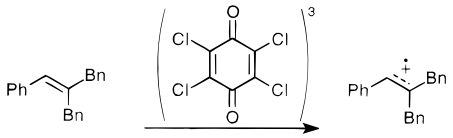

4

Laser photolysis of PTOC ester **10** gave radical **1**, which has no prominent chromophore at wavelengths greater than 300 nm, and the byproduct radical **5**. UV spectra obtained immediately after photolysis showed the absorbance of radical **5** and strong bleaching centered at 360 nm due to destruction of the PTOC ester. As radical **1** reacted, a strong signal centered at about 350 nm evolved in all solvents studied. Figure 3A shows a representative time-resolved spectrum obtained in acetonitrile. The initial spectrum was subtracted from subsequent spectra to remove the features produced immediately upon photolysis. The UV absorbances from the products evolving with time are positive signals, and the negative signal with λ_{max} at 490 nm is due to decay of radical **5**.

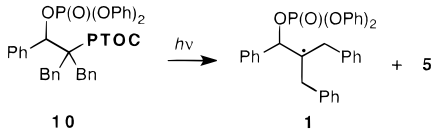

10 **1**

The spectrum in Figure 3A is a composite of signals from two species. The strong absorbance with λ_{max} at 354 nm is due to allylic radical **3**. In addition, a signal with λ_{max} at ~320 nm (from benzylic radical **2**) is present. The signal from **2** was more apparent in time-resolved spectra from reactions of **1**-d_{14}. Figure 3B shows the results from the deuterated radical obtained under the same conditions as used for the spectrum of the nondeuterated radical in Figure 3A. The 490 nm absorbances of radical **5** in A and B of Figure 3 were normalized so that the intensities of the signals between 300 and 370 nm could be compared directly to visualize yields. A and B of Figure 3 show the same period of reaction time (7.6 μs), and the rate constants for reactions of the two radicals are the same (see below). The difference in relative intensities of the 320 and 354 nm signals from the d_0 and d_{14} radicals demonstrates that at least two products are formed in reactions of radical **1** and that a KIE is present in at least one of the product-forming steps.

The kinetics of reactions of β-phosphatoxyalkyl radical **1** were measured in various solvents (Table S1 in Supporting Information), and Arrhenius functions were determined in THF and in acetonitrile (Table 1). A kinetic solvent effect was apparent with the rate constants increasing with solvent polarity, and the Arrhenius parameters indicate that this acceleration was due to a reduction in the activation energy. The precision in the kinetic measurements of first-order radical reactions with rate constants in the range of 10^4 s^{-1} is poorer than that for rate constants of ~10^5 s^{-1} because radical−radical reactions and reactions of radicals with residual oxygen are competitive with the slower processes, and we consider the rate constant measured in benzene (2×10^4 s^{-1} at 20 °C) to be an upper limit. The listed errors reflect the precision of the measurements, and the reproducibilities of values measured at the same temperature were good. Rate constants were the same for cases in THF where the kinetics were determined at both 320 and 358 nm showing that the two products formed came from the same precursor and were not subject to secondary reactions on the time scales of their formation. The reduced precision in the rate constants measured in THF and the limited temperature range over which the reactions could be studied in THF led to reduced precision in the Arrhenius functions in that solvent in comparison to those for reactions in acetonitrile.

Rate constants and Arrhenius parameters for reactions of **1**-d_{14} were also obtained in THF and acetonitrile (Tables S1 and 1). In regard to the overall rate constants of the reactions, there was no apparent (KIE). However, a KIE was present in the product distributions as is clear from the spectra in Figure 3.

Attempts to determine the ratios of product **2** to product **3** from the signal intensities at 320 and 354 nm were complicated by the relatively strong absorbance of radical **3** at 320 nm. Therefore, we estimated the amount of radical **3** produced in reactions in acetonitrile by an alternative approach. The relative intensities of the absorbances at 354 nm (from radical **3**) and at 490 nm (from radical **5**) from reactions of **1** in acetonitrile were compared to the relative intensities of these two absorbances observed when allylic radical **3** was produced from its PTOC ester precursor **12**. These comparisons gave the percentages of **3** formed in reactions of **1**-d_0 and **1**-d_{14}, and the remainder of the product was assumed to be radical **2**. From these analyses, the ratio of **2**:**3** from reaction of **1**-d_0 at 20 °C was 40:60 and

(16) Rathore, R.; Hubig, S. M.; Kochi, J. K. *J. Am. Chem. Soc.* **1997**, *119*, 11468−11480.

(17) Andre, J. J.; Weill, G. *Mol. Phys.* **1968**, *15*, 97−99.

Table 1. Arrhenius Parameters for Radical Reactions

radical	solvent	Arrhenius function[a]	k_{20} (s^{-1})[b]
1	THF	$(11.6 \pm 0.9) - (9.6 \pm 1.2)/\theta$	3×10^4
	CH_3CN	$(11.9 \pm 0.2) - (8.5 \pm 0.3)/\theta$	4×10^5
1-d_{14}	THF	$(10.8 \pm 0.4) - (8.4 \pm 0.6)/\theta$	3×10^4
	CH_3CN	$(12.2 \pm 0.2) - (8.8 \pm 0.3)/\theta$	4×10^5
1M	benzene[c]	$(12.1 \pm 0.6) - (8.1 \pm 0.9)/\theta$	1.1×10^6
	THF[d]	$(10.9 \pm 0.3) - (6.2 \pm 0.5)/\theta$	1.9×10^6
	CH_3CN[d]	$(11.0 \pm 0.5) - (5.0 \pm 0.7)/\theta$	1.8×10^7
13	THF[d]	$(10.7 \pm 0.5) - (6.2 \pm 0.6)/\theta$	1.2×10^6
	CH_3CN[d]	$(11.2 \pm 0.3) - (5.9 \pm 0.4)/\theta$	6×10^6

[a] Errors at 2σ, $\theta = 2.3RT$ in kcal/mol. [b] Calculated rate constant at 20 °C. [c] See ref 27. [d] See ref 7.

that from reaction of **1**-d_{14} was 70:30. We note that the ratio of products for reaction of **1** found in the approach used here differs from that we previously estimated from signal intensities at 320 and 354 nm,[6] but we believe the method used here is more reliable.[18] The change in the product ratio **2**:**3** does not necessarily translate directly to a KIE value because both reactions could have KIE, but if we assume that the rate of formation of the benzylic radical **2** is not affected by deuterium substitution, the KIE for formation of allylic radical **3** is $k_H/k_D = 3-4$.

The evolving spectra from reactions of radical **1** in acetonitrile and less polar solvents had no appreciable absorbance in the region 380−400 nm where radical cation **4** absorbs, and it is apparent that diffusively free **4** was not formed in detectable amounts. Radical **1** reacted rapidly in water/acetonitrile mixtures at ambient temperatures (submicrosecond lifetimes), and a signal from a new transient that we ascribe to **4** was observed in addition to the features seen in less polar solvents.

Figure 3C shows the time-resolved spectrum from reaction of **1** in 50% water (by volume) in acetonitrile. The time period in this figure is between 100 ns and 1.0 μs with the signals at 100 ns subtracted from later spectra to give a baseline. Growth of an absorbance at 390 nm was complete by 200 ns, and this signal is decaying in later spectra, whereas the absorbances between 300 and 370 nm are growing throughout. Similar behavior was observed in water solutions of 25 and 67%. The decaying absorbance in Figure 3C closely matches the UV spectrum of radical cation **4** in Figure 2D, and the observed kinetic behavior at 390 and 360 nm supports the assignment of the transient as **4**.[19]

The dynamics of the 390 nm signal were solved for double exponential behavior, first-order growth, and first-order decay, and the results are given in Table 2. The rate constants for the formation of this signal increased in a manner consistent with the expected trends in reactivity for radical **1** seen in less polar media. The pseudo-first-order rate constants for decay of the 390 nm signal are similar to those for reactions of styrene radical cations with alcohols reported by Johnston,[15] and we consider this to be good supporting evidence that the 390 signal is due to radical cation **4**.

The kinetic behavior of the signals in the 350−360 nm region from reactions in aqueous media was more informative. The

Table 2. Kinetics of Reactions of Radical **1** in Water/Acetonitrile Solutions at 22 ± 2 °C[a]

	25% water	50% water	67% water
390 nm growth	5.2 ± 1.0	9.4 ± 0.6 7.4 ± 0.8	14.7 ± 1.2
390 nm decay	3.3 ± 0.5	4.1 ± 0.2 4.6 ± 0.4	5.2 ± 0.5
360 nm first-order[b]	2.11 ± 0.02	3.03 ± 0.16	3.3 ± 0.4
360 nm k_1[c]	4.5 ± 2.8	7.1 ± 1.2	17 ± 2
360 nm k_2[c]	2.5 ± 0.2	2.1 ± 0.2	1.8 ± 0.2

[a] $10^{-6} \times k$ (s^{-1}); errors at 1σ. [b] First-order fit for growth at 360 nm. [c] Rate constants in Scheme 3.

Scheme 3

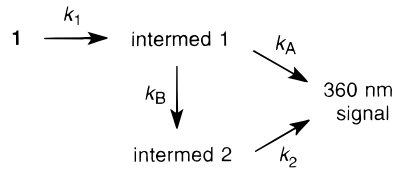

ratio of the ultimate signal intensity at 360 nm to the instantaneous signal intensity at 490 nm from byproduct radical **5** was essentially constant (ratios within 10%) in acetonitrile and the aqueous acetonitrile reactions, indicating that, irrespective of the formation of a new intermediate, the reactions eventually gave mainly allylic radical **3**. When the kinetics of growth in the 350−360 nm region were solved for a single-exponential rate law, rate constants in the range of $2-3 \times 10^6$ s^{-1} were obtained (Table 2). However, the precision of the first-order rate constants was increasingly poorer for increasing percentages of water, and inspection of the residuals from the "best first-order fit" of the traces suggested that the rate of formation was more complex than a first-order exponential process. Attempts to solve the data by the model of consecutive first-order reactions did not improve the fits; the regression analyses consistently converged to solutions in which one rate constant was very large ($\sim 10^8$ s^{-1}) and the other was $2-3 \times 10^6$ s^{-1}.

In the Discussion, we will argue that **1** reacts by initial heterolysis to give a contact ion pair that can react to give **2** and **3** or, in aqueous solutions, diffuse apart to give **4**. If this is the case, then **3** could be formed by two processes in aqueous acetonitrile media, reaction within the contact ion pair and deprotonation of diffusively free radical cation **4** by water. The kinetics could be complex with double exponential growth behavior of a first-order reaction combined with consecutive first-order reactions, although the data treatment is simplified somewhat by the fact that the rate constant for the slow initial reaction (the heterolysis) would be both the rate constant for the first-order process and that for the first step in the consecutive reaction sequence. Thus, the data traces for the signals in the 350−360 nm region were solved for the model shown in Scheme 3 where k_A, $k_B \gg k_1$. Inspection of the residuals for these data analyses indicated that the solutions were better than those for either of the other data treatments, but any double exponential solution would have given an improvement over the fits of the other data treatments. More importantly, the variable rate constants for the initial reaction ultimately giving the 350−360 nm signal (k_1 in Scheme 3) were essentially equal to those for the *formation* of the 390 nm signal, albeit at poorer precision, and the second rate constants in the consecutive reaction sequence (k_2) were similar to those for signal decay at 390 nm (Table 2). The data analyses also provided ratios for the partitioning of the initially formed intermediate (i.e., k_A/k_B) which indicated that the major reaction pathway to the 350−

(18) Qualitatively, the spectra from reactions of **1**-d_0 and **1**-d_{14} in THF were similar to those observed in acetonitrile. Quantitative measurements of the ratios of products by the method used for the product ratios in acetonitrile were not possible because the overall reactions were too slow in THF. Depletion of radicals by competitive radical−radical reactions in THF would lead to overestimation of the amounts of radical **2**.

(19) An experiment in an aqueous acetonitrile solution reported in our preliminary communication (ref 6) gave the same pseudo-first-order rate constant for growth at 360 nm as found here, but the temporal resolution in that experiment was not adequate for detection of the fast signal growth at 390 nm. The kinetic results in this work for aqueous solutions were obtained with a fast oscilloscope using 0.5 or 1.0 ns resolution.

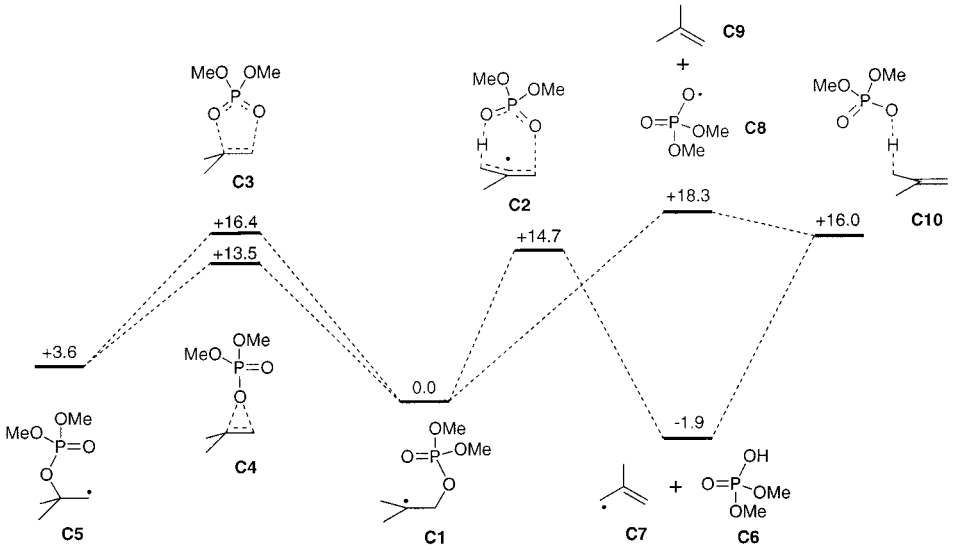

Figure 4. Potential energy surface for reactions of the 1,1-dimethyl-2-(dimethylphosphatoxy)ethyl radical (**C1**) as calculated at the Becke3LYP/6-311+G(d,p)//Becke3LYP/6-31G(d) + ΔZPE level of theory.

360 nm signal was the direct formation route (60−70%). Because the consecutive reactions sequence is the minor pathway and because decay of the transient absorbing at 390 nm would have a minor effect on the observed signal in the 350−360 nm region, the differences in values between k_2 from Scheme 3 and the rate constant for decay of the 390 nm signal seem to be acceptable.

Computational Studies. Previous computational results demonstrated that low-energy concerted pathways for migrations and eliminations of β-phosphatoxyalkyl radicals existed. Because radical **1** reacts by both migration and elimination, we have analyzed the reactions of a model radical that has both reaction channels available, the 1,1-dimethyl-2-(dimethylphosphatoxy)ethyl radical (**C1**), which represents a reasonable compromise between our desire to compute barriers at high levels of theory and the large number of heavy atoms in radical **1**. All barriers obtained for radical **C1** should be higher than those in radical **1** due to the phenyl group substitutions in **1**.

Three concerted reaction pathways for **C1** were explored (Figure 4), [1,3]-elimination through TS **C2** to give allyl radical **C7**, and [3,2]- and [1,2]-migrations through TS **C3** and **C4**, respectively, to give radical **C5**. Heterolytic fragmentation of **C1** was not addressed computationally in this study due to the lack of a reliable solvent model, but a stepwise homolytic fragmentation of **C1** followed by hydrogen atom transfer was studied. Energies of the stationary points are listed in Table 3.

In line with earlier studies of phosphatoxy rearrangements in smaller systems,[8] the barrier for the [1,2]-migration is lower than that for the [3,2]-shift, although the additional methyl groups in **C1** compared to the nor-methyl analogue lower the absolute reaction barriers significantly. Charge separation occurs in both pathways with cumulative charges on the dimethyl phosphate groups of −0.47 e in **C3** and −0.42 e in **C4** that are significantly larger than that for the phosphate group in precursor **C1** (−0.33 e) and product **C5** (−0.36 e). The product of migration, primary radical **C5**, is less stable than the tertiary radical **C1** by 3.6 kcal/mol which agrees well with previously estimated radical stabilization energies of approximately 2 kcal/mol for each methyl group.[20]

Table 3. Relative Energies (in kcal/mol) for Stationary Points in Concerted Reactions of **C1**

structure	ΔE[a] [B3LYP/ 6-31G(d)]	ΔE_0[b] [B3LYP/ 6-31G(d)]	ΔE[c] [B3LYP/ 6-311+G(d,p)// B3LYP/ 6-31G(d)]	ΔE_0[d] [B3LYP/ 6-311+G(d,p)// B3LYP/ 6-31G(d)]
C1	0.0	0.0	0.0	0.0
C2	+24.1	+19.6	+19.3	+14.7
C3	+19.5	+18.5	+17.4	+16.4
C4	+17.3	+15.9	+14.9	+13.5
C5	+5.0	+4.0	+4.6	+3.6
C6 + **C7**	+10.2	+6.9	+1.4	−1.9
C8 + **C9**	+23.3	+20.8	+20.7	+18.3
C10	+23.8	+19.9	+19.9	+16.0
C11	+22.7	+20.6	+20.4	+18.3

[a] ΔE_{tot}(Becke3LYP/6-31G(d)//Becke3LYP/6-31G(d)). [b] ΔE_{tot}(Becke3LYP/6-31G(d)//Becke3LYP/6-31G(d) + ΔZPE(Becke3LYP/6-31G(d)). [c] ΔE_{tot}(Becke3LYP/6-311+G(d,p)//Becke3LYP/6-31G(d)). [d] ΔE_{tot}(Becke3LYP/6-311+G(d,p)//Becke3LYP/6-31G(d) + ΔZPE(Becke3LYP/6-31G(d)).

The concerted elimination through TS **C2** is similar to that found in smaller systems.[8] Despite concertedness, the process is highly asynchronous as C−O bond cleavage is essentially complete in **C2** while proton transfer from carbon to oxygen has just begun (Figure S1 in Supporting Information). The phosphate group in **C2** carries a partial negative charge of −0.51 e excluding and of −0.16 e including the migrating hydrogen atom, highlighting the polar character. The activation energy is only 1.3 kcal/mol higher than that for the [1,2]-migration, indicating a close competition between elimination and rearrangement. The elimination reaction is slightly exothermic and thermodynamically favored over migration by 5.5 kcal/mol.

A transition state for homolytic C−O bond cleavage of **C1** could not be located, a finding in line with earlier results for elimination reactions of other electrophilic radicals.[21] From the total energy for homolysis (18.3 kcal/mol), this process is the least favorable addressed. A weakly bound complex, **C11**, between the phosphatoxy radical **C8** and isobutene (**C9**) exists, but the binding energy of 0.3 kcal/mol for **C11** is so small that differences in zero point vibrational energy are sufficient to yield a nonbonding interaction. Starting from **C11**, transition state **C10** for hydrogen transfer from isobutene to the phosphatoxy

(20) Viehe, H. G.; Janouske, Z.; Merenyi, R. *Substituent Effects in Organic Chemistry*; Reidel: Dordrecht, 1986. Pasto, D. J.; Krasnansky, R.; Zercher, C. *J. Org. Chem.* **1987**, *52*, 3062−3072.

(21) Engels, B.; Peyerimhoff, S. D. *J. Phys. Chem.* **1989**, *93*, 4462−4470. Engels, B.; Peyerimhoff, S. D.; Skell, P. *J. Phys. Chem.* **1990**, *94*, 1267−1275.

radical was located, but **C10** is more stable than complex **C11** by 2.3 kcal/mol, again due to zero point energy corrections. The partial negative charge of the phosphate group in **C10** is −0.33 e excluding the migrating hydrogen atom, the least polarized reaction addressed, and TS **C10** describes a typical homolytic process.

KIEs were calculated for processes shown in Figure 4 according to eq 1

$$\frac{k_{h6}}{k_{d6}} = \exp\left\{\frac{(\Delta G_{d6}^{\ddagger} - \Delta G_{h6}^{\ddagger})}{RT}\right\} \quad (1)$$

for reactant **C1** containing CD_3-substituents at the radical center. Inverse secondary KIEs of 0.79 and 0.83, respectively, were found for the [3,2]- and [1,2]-rearrangement reactions. The two phosphate elimination pathways have different KIEs as expected. The *syn*-1,3-elimination through **C2** has a large normal KIE of 4.51, whereas homolytic C−O bond cleavage to give **C8** and **C9** shows only a small inverse equilibrium isotope effect of 0.87. Under the condition that C−O bond fragmentation alone is rate limiting, formation of the 1,3-elimination products through a stepwise process will show only small isotope effects.

Insight into solvent effects on the reactions in Figure 4 was provided from evaluation of the dipole moments in the ground and transition states. Dipole moments of 0.88, 2.26, 2.31, and 2.64 D were calculated for structures **C1**, **C2**, **C3**, and **C4** in the gas phase, and the polarized transition states **C2**−**C4** will be stabilized relative to minimum **C1** in polar solvents. To quantify this expectation to some extent, we calculated the solvation energies of structures **C1**−**C4** using a simple Onsager solvation model which provides an approximation of the electrostatic component of the free energy of solvation. Solvent effects on the reaction barriers calculated for benzene, THF, acetonitrile, and water (Table S2 in Supporting Information) are modest in all cases. The [3,2]-shift through TS **C4** profits most from the presence of the solvent, and elimination through TS **C2** profits least. Most notably, however, the relative ordering of reaction barriers was not changed by solvent effects.

Discussion

β-Phosphatoxyalkyl radical reactions are a subset of *β*-ester radical reactions, a diverse collection that has received considerable attention due to their synthetic utility and the biological significance of the *β*-phosphate DNA radicals.[2] A comprehensive recent review of the general subject of *β*-ester radicals provides details of several mechanistic and computational studies of these reactions,[3] and some trends are apparent. One important generalization is that the reactions of *β*-acyloxyalkyl (*β*-carboxylate) radicals and *β*-phosphatoxyalkyl (*β*-phosphate) radicals are likely to be mechanistically related. Other generalizations concerning migrations and eliminations of *β*-ester radicals have emerged.

In the case of ester migration reactions, labeling studies and studies aimed at demonstrations of kinetic competence indicate that the migrations cannot involve diffusively free intermediates, either from heterolytic or homolytic cleavages, that recombine, nor can they proceed by initial 5-*endo* cyclizations followed by ring openings. Although fragmentations (either heterolytic or homolytic) followed by cage recombinations are not excluded by previous results, the conclusions based on labeling and computational work are that migrations occur mainly by a combination of open-shell concerted reactions, proceeding through three-center and five-center transition states as exemplified by **C3** and **C4** studied in this work. The *caveat*, however, is that most of the experimental work was performed in low-polarity solvents, and thus the conclusions might not be applicable to highly polar solvents.

In contrast to the above, the common view of elimination reactions of *β*-ester radicals is that they proceed by initial heterolysis to radical cations and anions, the model proposed by Schulte-Frohlinde in the earliest kinetic studies of such reactions.[22,23] A considerable amount of circumstantial evidence supports this view, including obvious polar characteristics in the transition states of the reactions[3] and product studies that require formation of common intermediates from isomeric reactants.[24] An especially compelling case for heterolysis of an α-oxy-*β*-phosphate radical to an enol ether radical cation in methanol was reported by Rist, Giese, and co-workers who observed CIDNP signals in the enol ether product.[25] Nevertheless, much of the evidence supporting heterolysis does not necessarily exclude other reactions; for example, few authors have considered the possibility that the results might be consistent with concerted elimination and nucleophilic substitution reactions. In addition, most of the elimination studies were performed in high-polarity media.

The differences in solvent polarities for studies of migrations and eliminations of *β*-ester radicals have left open the possibility that two distinctly different reaction mechanisms are involved for the two reactions. That explanation is in conflict with the results of LFP kinetic studies of radical **1** as well as radical **1M**, which reacts exclusively by phosphate migration to give **2M**, and radical **13**, which gives **14** by trifluoroacetate migration.

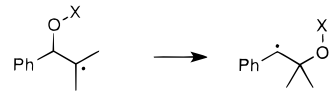

1M: X = P(O)(OPh)$_2$ **2M:** X = P(O)(OPh)$_2$
13: X = C(O)CF$_3$ **14:** X = C(O)CF$_3$

Because small concentrations of precursors are used in LFP studies, a wide range of solvents is acceptable. Radical **1** reacted by *both* migration and elimination reactions, and the two pathways were competitive in solvents of either low or high polarity. Consistent entropic factors (the log *A* term of the Arrhenius functions in Table 1) were found in THF and acetonitrile for radical **1,** suggesting that the mechanism is not altered by solvent polarity. A plot of the kinetics of reactions of **1** in various solvents at 20 °C against the $E_T(30)$ solvent polarity scale[26] (Figure 5) strongly reinforces this conclusion; a polarized transition state for a reaction pathway unaltered by solvent polarity changes is implicated by the well-correlated regression fit.[27] The trifluoroacetate migration in radical **13** also has similar log *A* terms in both THF and acetonitrile,[7] and, for radical **1M**, the entropies of activation were essentially constant in benzene, THF, and acetonitrile.[6,7,28] An important point is

(22) Behrens, G.; Koltzenbrug, G.; Ritter, A.; Schulte-Frohlinde, D. *Int. J. Radiat. Biol.* **1978**, *33*, 163−171.
(23) Koltzenburg, G.; Behrens, G.; Schulte-Frohlinde, D. *J. Am. Chem. Soc.* **1982**, *104*, 7311−7312.
(24) Peukert, S.; Giese, B. *Tetrahedron Lett.* **1996**, *37*, 4365−4368.
(25) Gugger, A.; Batra, R.; Rzadek, P.; Rist, G.; Giese, B. *J. Am. Chem. Soc.* **1997**, *119*, 8740−8741.
(26) Reichardt, C. *Chem. Rev.* **1994**, *94*, 2319−2358. Skwierczynski, R. D.; Connors, K. A. *J. Chem. Soc., Perkin Trans. 2* **1994**, 467−472.
(27) Using single weighting for each solvent or mixture of solvents and excluding the results in benzene, the slope of the regression line is 0.128 ± 0.003, and $r^2 = 0.998$.
(28) Horner, J. H.; Newcomb, M., unpublished results.

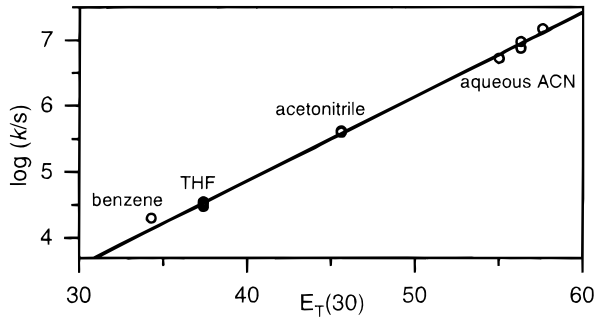

Figure 5. Measured rate constants for reactions of radical **1** in the 20−22 °C range as a function of the $E_T(30)$ solvent polarity terms. Multiple values in THF and in acetonitrile overlap one another. The limiting value for the rate constant for reaction in benzene was excluded from the regression line.

that the log *A* terms for phosphate migration in radical **1M** and trifluoroacetate migration in **13** are quite similar to those for the predominant phosphate elimination in radical **1**. From these behaviors, we infer that the migration and elimination reactions must be quite closely related. If this deduction is correct, the mechanistic question reduces to which pathway is involved, a common intermediate formed heterolytically or similar concerted processes.

The agreement between the relative barrier heights for migration and elimination found computationally for radical **C1** and the observation that the two processes are competitive in reactions of radical **1** might suggest that **1** reacts by concerted processes. However, the kinetic data for reactions of **1**-d_0 and **1**-d_{14} cannot be reconciled with such a conclusion. The overall rate constants for the reactions of these two radicals are indistinguishable, and the LFP measurements of the first-order processes are precise enough such that the differences in the rate constants for the two radicals cannot be greater than 10%. The large primary KIE found computationally for elimination in radical **C1** might be attenuated somewhat in radical **1** due to an earlier transition state, but it will not be lost completely. The inverse secondary KIE computed for concerted migrations of **C1** translates into an acceleration of the migration reaction of the deuterated radical, but this effect is much smaller than the primary KIE for the elimination and also should be attenuated in radical **1** somewhat due to an early transition state.

The observation of an isotope effect in the product ratios **2**:**3** combined with the lack of KIE in the overall rate constants is even more damaging to the position that the reactions are concerted because it demonstrates that transfer of a hydrogen atom or proton must occur *after* the rate-limiting step of the reaction. This is apparent in the spectra shown in A and B of Figure 3 for reactions of **1**-d_0 and **1**-d_{14}, respectively, in acetonitrile. These spectra display signal evolution over the same amount of time for reactions that had the same overall rate constants, but it is clear that allylic radical **3** was formed from **1**-d_{14} less rapidly than from **1**-d_0.

We conclude that radical **1** gives products **2** and **3** from a common intermediate that is produced in the rate-limiting step. The initial process must be a fragmentation, and the fragmentation apparently is heterolytic to account for the kinetic solvent effects found here and observed in other β-ester radical reactions.[3]

Radical cation **4** was not produced in nonreactive solvents where it could have been observed easily. In a similar manner, no radical cation was detected in THF or acetonitrile reactions of radical **1M** which reacts more than an order of magnitude faster than **1** and which gives only the benzylic radical product **2M** that has no appreciable absorbance at wavelengths greater than 330 nm. The detection of **4** in the reactions of radical **1** in water/acetonitrile mixtures obviously supports a heterolysis pathway, but it is the observed kinetic behavior in aqueous acetonitrile solutions that provides a more compelling argument for heterolysis. In these solutions, a common intermediate for diffusively free radical cation **4** and allylic radical **3** is implicated by the agreement in the rate constants for formation of both species (Table 2).

Scheme 4

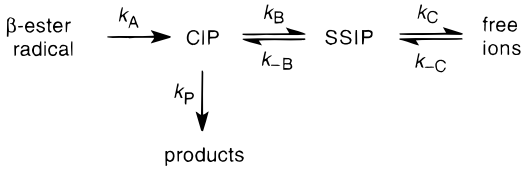

The reactions of radical **1** can be cast in a model that is the same as that for heterolysis of a closed-shell species reacting in a solvolysis reaction (Scheme 4). The first-formed species is a contact ion pair (CIP) which can react in various modes or proceed to a solvent-separated ion pair (SSIP). In turn, the SSIP can collapse back to the CIP or separate further to give the diffusively free ions, and some reactions, such as electron transfer, might occur in the SSIP. Sprecher proposed that such a scheme was consistent with the reaction diversity in an overview of β-ester radical reactions.[29]

The occurrence of two types of ion pairs is not required to explain the kinetics of radical **1**. The reaction pathway in aqueous acetonitrile could involve a single intermediate that partitions, and failure of that intermediate to partition in less polar media would explain the absence of radical cation formation. Nevertheless, contact pairs involving radical cations apparently behave as encounter complexes that evolve to solvent-separated pairs with diffusion-like rate constants, on the order of 10^9-10^{10} s^{-1}.[16,30] If the CIP from radical **1** solvates this rapidly, then another ion pair (the SSIP) provides a reservoir for the radical cation that can partition back to the CIP in competition with dissociation to give free ions. The ratio of rate constants for dissociation of the SSIP and collapse back to the CIP is likely to be highly sensitive to solvent effects with relatively small rate constants for dissociation in nonpolar media that preclude formation of diffusively free ions in detectable amounts.

The dynamics of some of the processes occurring in the CIP can be deduced in a semiquantitative sense. For example, fast proton transfer within a CIP containing **4** must have occurred in the photoejection experiments conducted in this work. Photoejection produces the CIP of the styrene radical cation and a solvated electron, in this case the radical anion of acetonitrile. Despite the favorable energetics for back electron transfer to return the neutral styrene, which is likely to be a major reaction, some escape from the CIP occurred with the β,β-dimethylstyrene radical cation to give the diffusively free radical cation **4M** that was detected. When a similar experiment was attempted with β,β-dibenzylstyrene, however, the major product observed "instantly" on the nanosecond time scale apparently was allylic radical **3** instead of radical cation **4**. Therefore, the deprotonation of **4** by the acetonitrile radical anion

(29) Sprecher, M. *Chemtracts: Org. Chem.* **1994**, *7*, 115−119.
(30) Arnold, B. R.; Noukakis, D.; Farid, S.; Goodman, J. L.; Gould, I. R. *J. Am. Chem. Soc.* **1995**, *117*, 4399−4400.

apparently was faster than the overall escape process in this experiment.

Deprotonation of **4** by the phosphate anion to give **3** and collapse of the ions to give **2** within the CIP formed from radical **1** also must to be quite fast.[31] The kinetic model for reactions of **1** in aqueous acetonitrile indicated that the major reaction pathway was direct formation of allylic radical **3**, and the partitioning appeared to be relatively constant in water solutions of 25, 50, and 67% with the direct reaction amounting to 60−70% of the total reaction. If evolution of the CIP to the SSIP is nearly diffusion-limited, the constant partitioning ratio with increasing water content would require either that deprotonation and collapse were competitive with SSIP formation or that the rate of separation of the SSIP to free ions was not sensitive to solvent polarity. The latter option is inconsistent with the absence of free ions when acetonitrile and less polar solvents were employed.

It might be instructive to note why we originally believed[6] that the results with radical **1** indicated that the reactions involved concerted processes. A radical cation intermediate was not observed in the original work,[19] thus obviating any demonstration of kinetic competence. The negative entropies of activation for reaction of **1** and related radicals appear to be inconsistent with an initial heterolysis reaction; we can only rationalize these at this time as resulting from highly organized transition states for heterolysis, such as shown in **15**, with several orbitals in the incipient radical cation co-aligned and the ester group in a stereoelectronically favorable orientation. Finally, the high degree of stereochemical integrity in phosphate migrations of radicals similar to radical **1**[5,32] suggested concerted mechanisms, although the results can be accommodated in the context of ion pair formation if collapse is exceedingly fast.

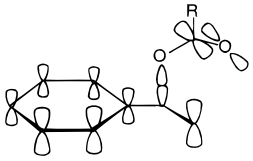

15

The CIDNP study of phosphate elimination to give an enol ether radical cation in methanol[25] and the results of this work provide direct spectroscopic confirmation of heterolysis reactions in polar media, and the present results indicate that the mechanism of reaction of radical **1** is the same in less polar media. Accordingly, heterolysis appears to be the common pathway for reactions of β-phosphatoxyalkyl radicals when the incipient radical cation is at least as stable as those from enol ethers and styrenes.[33] Studies aimed at further characterization of these reactions might focus on the putative ion pairs, the reactions of which should be highly solvent-dependent.[34] Whether or not the relatively low-energy concerted processes found computationally for radical **C1** in this work and previously for similar β-phosphate alkyl radicals[8] are important when such stable radical cations cannot be formed remains an open question. That question probably will not be resolved by the methods used in this work because diffusively free radical cations apparently are not formed in reactions of simple β-ester radicals even in water.[23]

Experimental Section

Syntheses: described in the Supporting Information.

Laser Flash Photolysis. LFP studies were performed with an Applied Photophysics LK-50 kinetic spectrometer using a Nd:YAG laser for 266 nm (photoejection studies) or 355 nm (PTOC ester and chloranil studies). All studies were performed with dilute, He-sparged (unless noted) flowing solutions of precursor. Temperatures were controlled by circulating a bath solution through the jacket of the storage funnel, and temperatures were measured with a thermocouple placed in the flowing stream immediately above the irradiation region of the flow cell. For reactions in acetonitrile/water mixtures, syringe drive pumps were used with gas-tight syringes containing a solution of PTOC ester precursor in acetonitrile in one syringe and water or water/acetonitrile in a second syringe; the solutions were mixed in a tee located immediately before the flow cell, and LFP experiments were performed within 5 s of mixing.

Kinetic Data Analyses. For kinetic runs, several traces typically were averaged to improve signal-to-noise. First-order analyses were performed with the Applied Photophysics software. Double exponential analyses and analyses for the complex kinetic scheme in Scheme 3 were performed with Sigmaplot software. For the kinetic analysis of Scheme 3, eq 2 was fit

$$\mathrm{Abs} = p_1 + p_2 \exp(-k_1 t) + (p_3/(k_2 - k_1))((k_2(1 - \exp(-k_1 t))) - (k_1(1 - \exp(-k_2 t)))) \quad (2)$$

where p_n are variable absorbance terms, k_n are variable rate constants, and Abs is the observed absorbance at time t. The ratio p_2/p_3 from eq 2 gives the ratio k_A/k_B in Scheme 3, assuming that a common species is formed from both pathways.

Computational details. Geometry optimizations were performed at the UHF/3-21G(d) level of theory and with the hybrid UBecke3LYP/6-31G(d) density functional, or B3LYP/6-31G(d), method[35] as implemented in Gaussian 94.[36] A large number of conformers were optimized for radicals **C1** and **C5** at the UHF/3-21G(d) level of theory. The three most favorable conformers of each radical were then reoptimized at the B3LYP/6-31G(d) level. All stationary points were characterized through calculation of analytical second derivatives. Improved relative energies for the stationary points characterized at this level of theory were then calculated using the larger 6-311+G(d,p) basis set at the UBecke3LYP level of theory. Thermochemical quantities were calculated from the unscaled harmonic vibrational frequencies at 293.15 K and are composed of relative energies at the Becke3LYP/6-311+G(d,p)//Becke3LYP/6-31G(d) level of theory and thermochemical corrections derived from the Becke3LYP/6-31G(d) frequencies. KIEs were calculated from free energy differences between isotopomers. As in earlier studies,[8] partial charges were obtained from the Mulliken population analysis of the Becke3LYP/6-31G(d) Kohn−Sham orbitals. Solvent effects were estimated with a simple Onsager reaction field

(31) An alternative to two-electron processes within the CIP of radical cation **4** and phosphate anion is possible. Electron transfer in the CIP of **4** and diphenyl phosphate anion would give the styrene and a phosphatoxyl radical which will be quite reactive. For example, our computational results indicated that the transition state for H-atom transfer from isobutene to the dimethylphosphatoxyl radical was *lower* in energy than the weakly bound ensemble.

(32) Crich, D.; Escalante, J.; Jiao, X. Y. *J. Chem. Soc., Perkin Trans. 2* **1997**, 627−630.

(33) Ethyl vinyl ether and styrene have the same oxidation potentials in acetonitrile. See: Katz, M.; Riemenschneider, P.; Wendt, H. *Electrochim. Acta* **1972**, *17*, 1595−1607.

(34) Following the submission of this work, we found a β-phosphatoxyalkyl radical that reacts by heterolytic cleavage resulting in phosphate migration and/or formation of diffusively free radical cation as a function of solvent polarity. See: Whitted, P. O.; Horner, J. H.; Newcomb, M.; Huang, X.; Crich, D. *Org. Lett.* **1999**, *1*, 153−156.

(35) Becke, A. D. *J. Chem. Phys.* **1993**, *98*, 5648−5652. Lee, C.; Yang, W.; Parr, R. G. *Phys. Rev. B* **1988**, *37*, 785−789. Hertwig, R. H.; Koch, W. *J. Comput. Chem.* **1995**, *16*, 576−585.

(36) Frisch, M. J.; Trucks, G. W.; Schlegel, H. B.; Gill, P. M. W.; Johnson, B. G.; Robb, M. A.; Cheeseman, J. R.; Keith, T.; Petersson, G. A.; Montgomery, J. A.; Raghavachari, K.; Al-Laham, M. A.; Zakrzewski, V. G.; Ortiz, J. V.; Foresman, J. B.; Cioslowski, J.; Stefanov, B. B.; Nanayakkara, A.; Challacombe, M.; Peng, C. Y.; Ayala, P. Y.; Chen, W.; Wong, M. W.; Andres, J. L.; Replogle, E. S.; Gomperts, R.; Martin, R. L.; Fox, D. J.; Binkley, J. S.; Defrees, D. J.; Baker, J.; Stewart, J. P.; Head-Gordon, M.; Gonzalez, C.; Pople, J. A. *Gaussian 94*, revision E.2; Gaussian, Inc.: Pittsburgh, PA, 1995.

model using a spherical cavity.[37] The dielectric constants used were as follows: benzene (2.27), THF (7.58), acetonitrile (35.9), and water (78.3).

Acknowledgment. We thank the National Institutes of Health (GM56511 to M.N. and CA60500 to D.C.), the National Science Foundation (CHE9625256 to D.C. and CHE9614968 to M.N.), and the Volkswagen-Stiftung (to H.Z.) for financial support. The work in Germany was supported by the Leibniz-Rechenzentrum München through computational resources. We thank Dr. S. -Y. Choi for experimental assistance.

(37) Wong, M. W.; Frisch, M. J.; Wiberg, K. B. *J. Am. Chem. Soc.* **1991**, *113*, 4776−4782.

Supporting Information Available: Kinetic results for reactions of **1**-d_0 and **1**-d_{14} in low polarity solvents, computed solvent effects, structures for ground and transition states for radical **C1**, and details of the synthetic reactions (PDF). This material is available free of charge via the Internet at http://pubs.acs.org.

JA991012R